Random Signal Digital Simulator Based on Its Double Chain Markov Model

Oleg V. Chernoyarov, Alexey N. Glushkov, Maksim Y. Kalinin, Kaung Myat San, and Vladimir P. Litvinenko

***Abstract*—The universal digital simulator of a random signal with the required three-dimensional probability distribution of its discrete values is introduced. The simulation algorithm is based on a double chain Markov model of the signal samples. Thus, at the simulator output, a sequence of binary codes of the samples with the required probabilistic and correlation properties of the three adjacent random or pseudo-random values is generated. A technique for determining the parameters of the double chain Markov model is considered. It is based either on the specified three-dimensional probability density or on the experimental sampling of a simulated random process. The block diagram for the hardware implementation of the simulator is proposed. It is built using microprocessors or field-programmable gate arrays that can provide a high sampling rate. It is shown that the computational procedure is simple and that it can be implemented using rather inexpensive typical components. The replacement of the model of the simulated random signals is carried out by either reloading the memory device by the pre-generated data array or by switching to memory pages where the necessary arrays are stored. The properties of the simulator including its probabilistic and correlation characteristics are studied. It is established that a high accuracy of coincidence between the theoretical three-dimensional probability distribution of the simulated model and the histogram built on the sequence of generated random signal samples is provided. It is also pointed out that the proposed simulator can be used in research, development and testing of electronic equipment of various purposes, including different measurers and radio path simulators.**

***Index Terms*—Random signal simulator, three-dimensional probability distribution, discrete values, Markov model, matrix of transition probabilities, estimate of parameter, statistical simulation**

Manuscript received November 18, 2020; revised August 20, 2021. This work was financially supported by the Ministry of Education and Science of the Russian Federation (research project No. FSWF-2020-0022) as well as the Russian Science Foundation (research project No. 20-61-47043)

O. V. Chernoyarov is a Professor at the Department of Electronics and Nanoelectronics, National Research University "MPEI", Moscow, Russia, on leave from the International Laboratory of Statistics of Stochastic Processes and Quantitative Finance, National Research Tomsk State University, Tomsk, Russia (e-mail: chernoyarovov@mpei.ru).

A. N. Glushkov is a Head of the Department of Infocommunication Systems and Technologies, Voronezh Institute of the Ministry of Internal Affairs of the Russian Federation, Voronezh, Russia (e-mail: al.nk.glushkov@gmail.com).

M. Y. Kalinin is a Director of the limited liability company "Impulse-Service", Moscow, Russia (e-mail: maks@oxrana.org).

Kaung Myat San is a PhD candidate at the Department of Electronics and Nanoelectronics, National Research University "MPEI", Moscow, Russia (corresponding author, phone: +7-495-362-71-68; fax: +7-495-362-89-38; e-mail: kautmyatsan@mail.ru)

V. P. Litvinenko is an Associate Professor at the Department of Radio Engineering, Voronezh State Technical University, Voronezh, Russia (e-mail: vl.pt.litvinenko@gmail.com).

I. Introduction

Simulators (generators) of random information or interference signals with the required multidimensional statistical properties are applied to solve various radio engineering problems, or to design, research and test radio equipment, or to control and monitor devices for simulating radio channels characterized by specific types of additive interferences and signal fading [1]-[5]. Besides, various systems are often analyzed using statistical modeling based on the random reference data [6], [7]. As a rule, common devices use sources of thermal noise or number generators with a uniform probability distribution [1], [8]. And then, in order to change the probabilistic properties of the generated sequence, functional transformations of samples are used. All of them have limited capabilities and, in addition, technical difficulties may arise during the implementation of the complex functional transformations, especially when providing the required multidimensional probabilistic properties [4], [5]. The generation of the random numbers with a distorted form of, for example, the Gaussian probability distribution [9] among others is of interest, as well as the generation of the random number sequences for the forecasting tasks [10] using the three-dimensional statistical relations of these sequences.

The introduced device uses a double chain Markov model of a random process [11], and it significantly expands the capabilities of the digital random signal simulator based on a simple chain Markov model [12], [13] allowing reproducing more complex internal statistical bonds. Its distinctive feature is a universality meaning that an unlimited sequence of samples with the varied three-dimensional probability distributions can be generated while the signal properties are changed by loading the corresponding pre-calculated data array into a memory device.

II. The Double Chain Markov Model

In the double chain Markov model [14]-[16] of a discrete random process with the integer samples s_n, where $n=\overline{1,N}$ is the number and N is the amount of sampling, the current value $s_n=k$ depends only upon the two previous values $s_{n-1}=j$ and $s_{n-2}=i$. Here $i,j,k=\overline{1,M}$

are the possible sample values and M is the general number of sample values. The model is described by the transition probabilities p_{ijk} forming the three-dimensional matrix $\left[p_{ijk}\right]$. This matrix can be graphically presented in the form of a cube, as it is shown in Fig. 1.

It is more convenient to represent the three-dimensional matrix $\left[p_{ijk}\right]$ in the form of the matrix which is the column of the two-dimensional matrices:

$$\left[p_{ijk}\right]=\left[\left[p_{ik}^{(1)}\right]\ \left[p_{ik}^{(2)}\right]\ \dots\ \left[p_{ik}^{(M)}\right]\right]^{\mathrm{T}}, \tag{1}$$

where T is the matrix transposition operation, $\left[p_{ik}^{(j)}\right]$ is the square matrix of transition probabilities that has the size of $M\times M$ while j is fixed,

$$\left[p_{ik}^{(j)}\right]=\begin{bmatrix} p_{1j1} & \dots & p_{1jM} \\ p_{2j1} & \dots & p_{2jM} \\ \dots & \dots & \dots \\ p_{Mj1} & \dots & p_{MjM} \end{bmatrix}. \tag{2}$$

Similarly to [15], by combining the samples $s_{n-1}=j$ and $s_{n-2}=i$ into the value

$$q=M(j-1)+i, \qquad q=\overline{1,M^2}, \tag{3}$$

the rectangular matrix of transition probabilities that are $M^2\times M$ by the size can be obtained in the form

$$\left[p_{qk}\right]=\begin{bmatrix} p_{11} & \dots & p_{1M} \\ p_{21} & \dots & p_{2M} \\ \dots & \dots & \dots \\ p_{M^2 1} & \dots & p_{M^2 M} \end{bmatrix}. \tag{4}$$

Based on the transition probabilities p_{ijk}, the probability distribution function F_{ijk} is calculated as follows

$$F_{ijk}=\sum_{r=1}^{k} p_{ijr}. \tag{5}$$

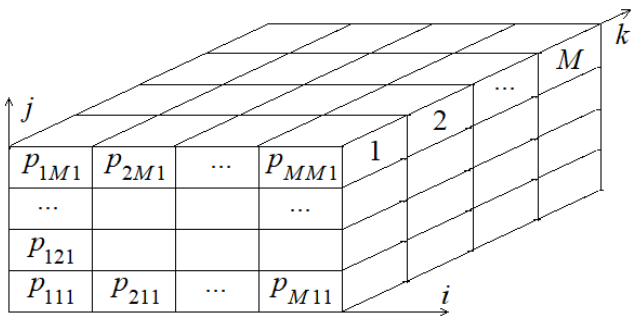

Fig. 1. The three-dimensional matrix of transition probabilities.

It can also be represented by a matrix in the format (1), (2) or (4). It should be noted that, when k increases, the values of F_{ijk} vary from $F_{ij1}=0$ to $F_{ijM}=1$.

III. Building the Double Chain Markov Model

To start with, it is presupposed that the three-dimensional probability density $w(x_1,x_2,x_3)$ of the sequential unquantized values $\tilde{s}_{n-2}$, $\tilde{s}_{n-1}$, $\tilde{s}_n$ of the simulated random process is already known. The random process is sampled at the intervals of time τ by an analog-to-digital converter (ADC) with the quantization step d and the quantization interval boundaries

$$c_r=(r-M/2)d+s_{\mathrm{mean}}, \qquad r=\overline{1,(M-1)}. \tag{6}$$

In (6), s_{mean} is the mean value of the random process, while the total number of intervals is $M=2^m$ and $c_1=-\infty$, $c_M=\infty$. The quantization step d is chosen depending upon the root-mean-square deviation of the random process. In this case, the joint probabilities of the values of discrete samples $s_{n-2}=i$, $s_{n-1}=j$, $s_n=k$ are equal to

$$p(i,j,k)=\int_{c_{i-1}}^{c_i}\int_{c_{j-1}}^{c_j}\int_{c_{k-1}}^{c_k} w(x_1,x_2,x_3)\,\mathrm{d}x_1\mathrm{d}x_2\mathrm{d}x_3, \tag{7}$$

while the transition probabilities are

$$p_{ijk}=\frac{\int_{c_{i-1}}^{c_i}\int_{c_{j-1}}^{c_j}\int_{c_{k-1}}^{c_k} w(x_1,x_2,x_3)\,\mathrm{d}x_1\mathrm{d}x_2\mathrm{d}x_3}{\int_{c_{i-1}}^{c_i}\int_{c_{j-1}}^{c_j}\int_{-\infty}^{\infty} w(x_1,x_2,x_3)\,\mathrm{d}x_1\mathrm{d}x_2\mathrm{d}x_3}, \tag{8}$$

respectively.

The experimental Markov model can be built for a sampling of the observed random process z_n, $n=\overline{1,L}$ at the ADC output. According to the values of this sampling, the numbers l_{ijk} of the transitions from a pair of previous values $z_{n-2}=i$ and $z_{n-1}=j$ to the current value $z_n=k$ are calculated, and thus the transition probabilities of the Markov model can be estimated in the following way [12], [13]:

$$p_{ijk}=l_{ijk}\Big/\sum_{r=1}^{M} l_{ijr}.$$

In order to eliminate possible zero values in the denominator of the expression (8), any small constant that may be 1, for example, should be added to the values of l_{ijk}.

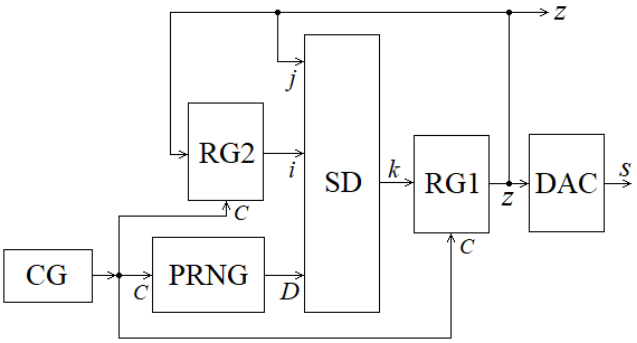

Fig. 2. The block diagram of the random signal simulator.

IV. The Block Diagram of the Simulator

The block diagram of the random signal simulator based on a double chain Markov model is shown in Fig. 2.

By the signals *C* passing from the clock generator (CG) with the frequency *f*, and in accordance with a uniform probability distribution, the pseudo-random (or random) number generator (PRNG) outputs the binary *r*-bit numbers, their decimal equivalent being D_n (*n* is the number of the current sample). The PRNG can be implemented by means of a noise random number generator [17], or through feedback shift registers [8] provided by the *M*-sequence generator, for example. It can be noted that the properties of the generated random numbers depend on the selected statistical characteristics of the PRNG, and to maintain the latter the methods described in [18] can be used.

In the storage device (SD), in the cells with the addresses

$$A = j \cdot 2^{r+m} + i \cdot 2^r + D, \quad r = \log_2 D > m, \quad m = \log_2 M, \quad i, j = \overline{0, M-1} \tag{9}$$

the least values of $k = \overline{0, M-1}$ are stored that have been pre-calculated for all $D = \overline{0, 2^r - 1}$ and for each pair of values of *i*, *j*, thus satisfying the inequalities

$$D/2^r \le F_{(i+1)(j+1)(k+1)} < (D+1)/2^r . \tag{10}$$

In the immediate CG cycle, the PRNG generates the number *D* and the binary code of the number *k* is read from the SD at the address *A* while the RG2 register is in the state *i* and the RG1 register is in the state *j*. In the next clock cycle, the value *k* is poked into the RG1 register so that it becomes the output code *z* of the random process. Then it is fed to the SD address input generating a new value of *j* and then it is saved in the RG2 register generating a new value of *i*. Further, the specified process is repeated. The sample sequence z_n is transformed by the digital-to-analog converter (DAC) into the random analog output signal.

V. The Normal Random Process Simulator

As an example, one now consider the simulator of a normal random process $s(t)$ with the specified three-dimensional probability density of the form [19], [20]

$$w(x_1, x_2, x_3) = \frac{1}{\sigma^3 \sqrt{(2\pi)^3 H}} \times \exp\left[-\frac{1}{2\sigma^2 H} \sum_{m=1}^{3} \sum_{n=1}^{3} H_{mn} (x_m - s_{\text{mean}})(s_n - x_{\text{mean}}) \right],$$

where s_{mean} is the mean value; σ is the root-mean-square deviation of the random process; $H = |[R_{mn}]|$ is the determinant of the normalized correlation matrix

$$[R_{mn}] = \begin{bmatrix} 1 & R_{12} & R_{13} \\ R_{21} & 1 & R_{23} \\ R_{31} & R_{32} & 1 \end{bmatrix}, \quad R_{mn} = R_{nm} = \langle [s(t_{l+m}) - s_{\text{mean}}][s(t_{l+n}) - s_{\text{mean}}] \rangle / \sigma^2 , \tag{11}$$

l is an arbitrary integer; and H_{mn} are the elements of the matrix inverse to the correlation matrix (11).

Having chosen the quantization step by the level $d = 8\sigma/M$ and after applying (6)-(8), one can now calculate the values of $p(i, j, k)$ (7) and p_{ijk} (8) that are the joint and the transient probabilities, respectively. These values can be conveniently represented by the rectangular matrices $[p(q,k)]$ and $[p_{qk}]$ of the form (4) and, as graphic images, by the three-dimensional diagrams within the coordinates (q,k). In Fig. 3a, one can see the diagram of the matrix $[p(q,k)]$, in Fig. 3b – its level lines, and in Fig. 3c – the diagram of the matrix $[p_{qk}]$. It is assumed that $s_{\text{mean}} = 0$, $\sigma = 1$, $M = 32$ ($m = 5$), $R_{12} = R_{21} = 0.1$, $R_{13} = R_{31} = 0.5$, $R_{23} = R_{32} = 0.2$. As it follows from Fig. 3, the surface $[p(q,k)]$ is multimodal and the slope of the surfaces in the plane (q,k) is determined by the correlation coefficients (11).

In Figs. 4, there are presented the examples of the three-dimensional diagrams demonstrating the matrices of the transition probabilities $[p_{ik}^{(j)}]$ (2) for different values of *j*. Their combination constitutes the diagram of the full matrix of the transition probabilities presented in Fig. 3c.

In Figs. 5, one can see the results of the calculation of the double chain Markov model referring to the same Gaussian random process with the decreased element $R_{13} = R_{31} = 0.3$ of the correlation matrix (11). As it can be seen, the three-dimensional diagrams of the double chain Markov models tend to change significantly. Thus, they allow revealing the changes in even only one of the correlation coefficients, that is, they can describe quite "fine" properties of the simulated random processes, while simple chain Markov

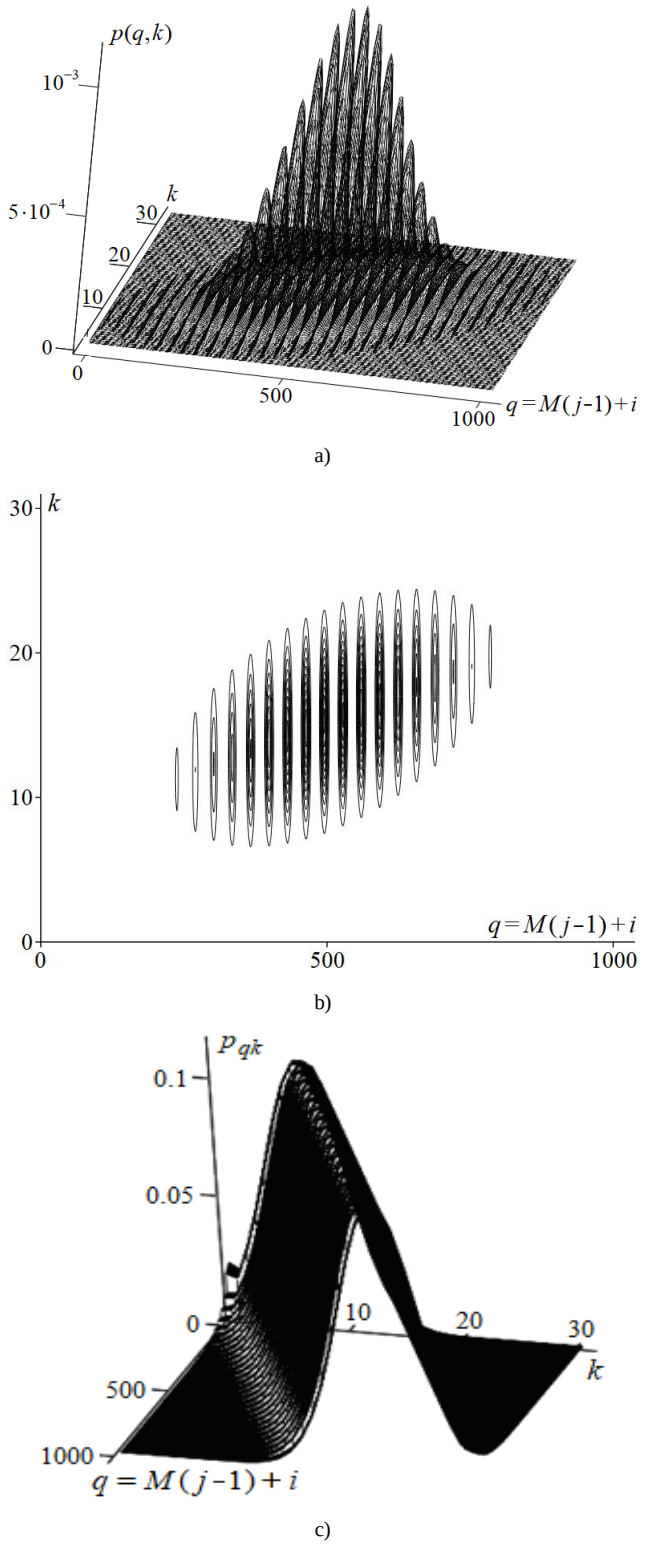

Fig. 3. The probability matrix diagrams.

models are not sensitive enough to the same kind of changes.

VI. Simulation of the Simulator Operation

In order to form the SD data array according to (10), the probability distribution function F_{ijk} (5) is used that should be represented by the two-dimensional array (matrix) of the form

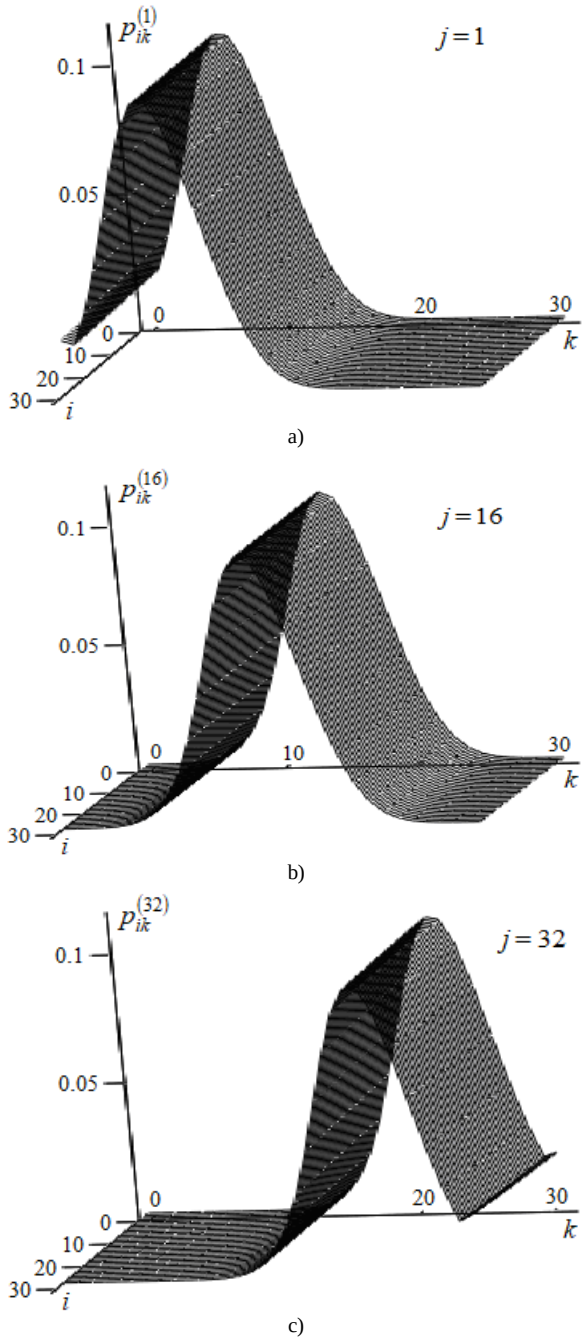

Fig. 4. The transition probability matrix diagrams.

$$F_{qk} = \sum_{r=1}^{k} p_{qr} ,$$

where $q = M(j-1)+i$, $i, j, k = \overline{0, M-1}$ while the inequalities (10) take the form

$$D/2^r \le F_{qk} < (D+1)/2^r . \qquad (12)$$

The example of the three-dimensional diagram of the matrix F_{qk} under $R_{12} = R_{21} = 0.1$, $R_{13} = R_{31} = 0.3$, $R_{23} = R_{32} = 0.2$ is shown in Fig. 6a. In Figs. 6b and 6c, the particular F_{qk} diagrams are plotted for $j = 0$ and $j = 31$; the combination of such diagrams constitutes F_{qk}. From (12), for all the sets of the numbers *i*, *j* and *D*, the least

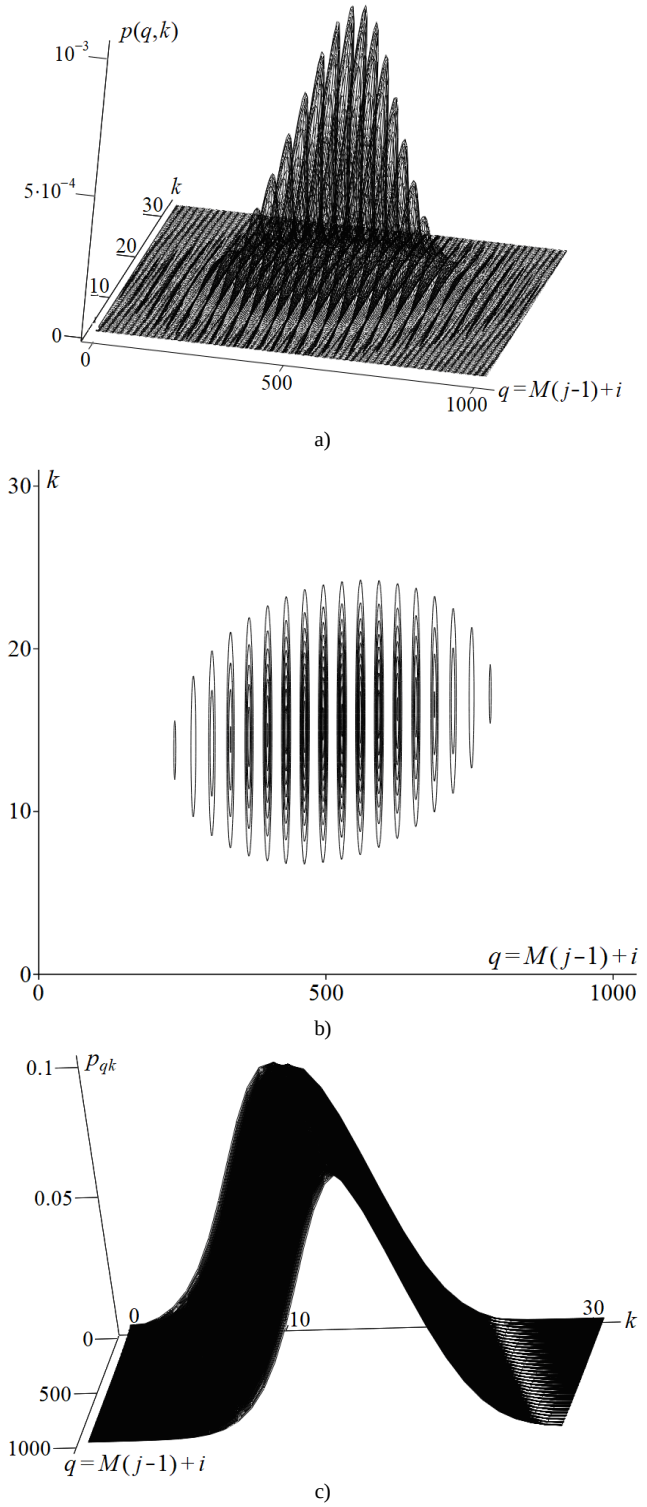

Fig. 5. The transition probability matrix diagrams.

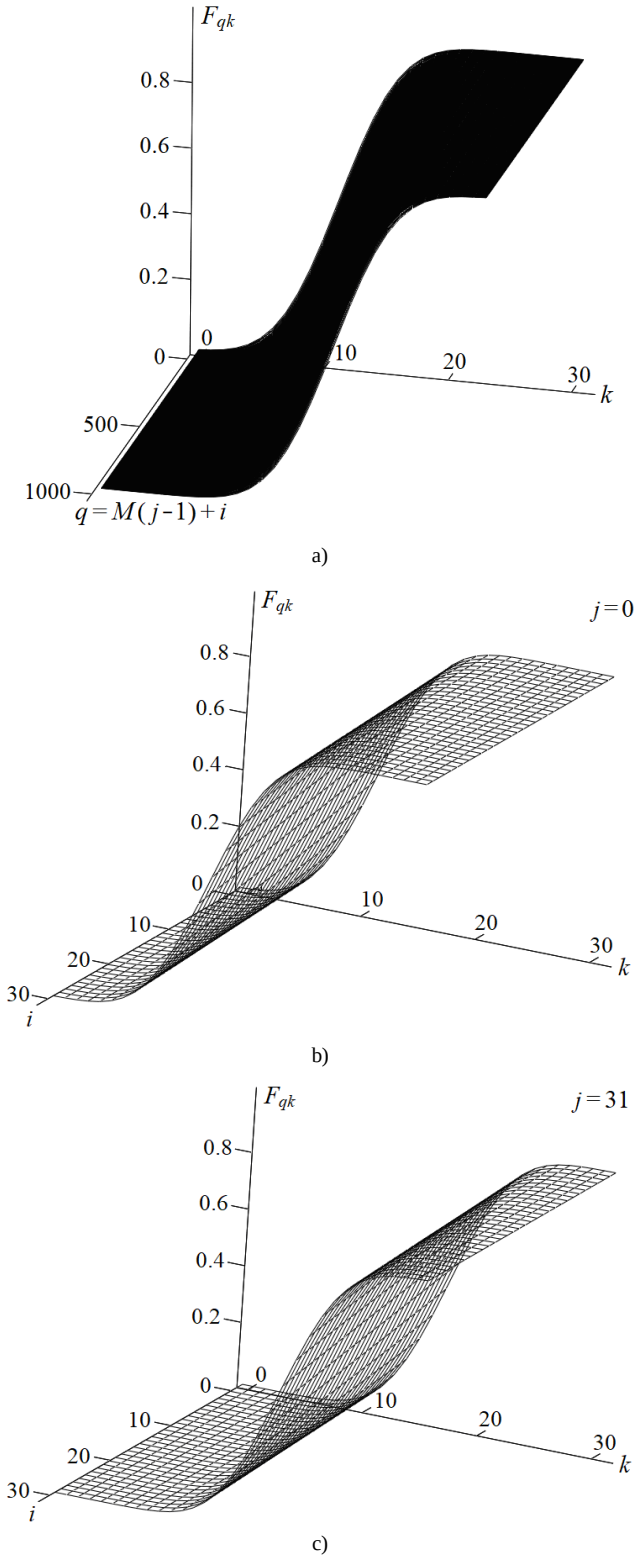

Fig. 6. The diagrams of the probability distribution functions of the Gaussian random process.

values of k are calculated, and further the latter are stored in the SD at the address A determined according to (9).

In accordance with the provided description, the statistical simulation of the simulator operation presented in Fig. 2 has been carried out. In Fig. 7, the time realizations of the random process samples z_{1n} (Fig. 7a) and z_{2n} (Fig. 7b) obtained as a result of the statistical simulation of the simulator operation. It is presupposed that the equality $R_{13} = R_{31} = 0.3$ is for the samples z_{1n} while the equality $R_{13} = R_{31} = 0.5$ is for the samples z_{2n}. All the other parameters have been specified above already.

By the realizations of the large-volume samples ($N > 10^6$), the statistical estimates of the joint probability distribution $p(q,k)$ can be obtained in the form

$$p(q,k) = l_{qk} \Big/ \sum_{q=0}^{M^2-1} \sum_{k=0}^{M-1} l_{qk}, \qquad (13)$$

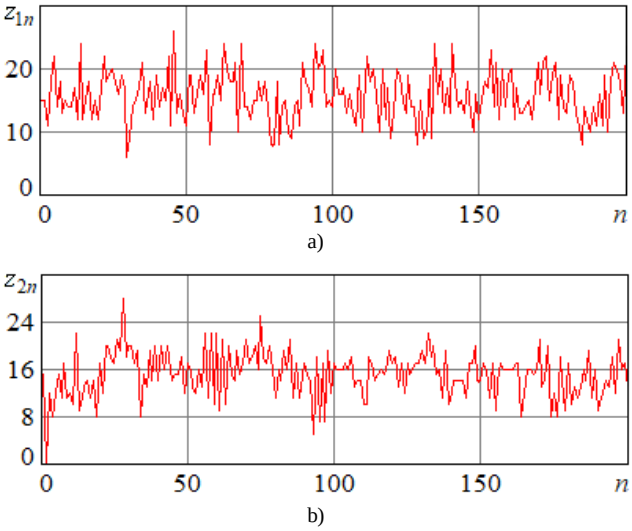

Fig. 7. The time realizations of the simulated Gaussian random processes with different correlation coefficients.

where l_{qk} is the number of the transitions of the sample values from $q = M(j-1)+i$ to k. The three-dimensional diagrams of $p(q,k)$ are shown in Fig. 8a (for the processes z_{1n}) and Fig. 8b (for the processes z_{2n}) and the corresponding level lines are plotted in Fig. 8c and Fig. 8d. The comparison of the experimental diagrams (Figs. 8) with the theoretical ones presented in Figs. 5a, 5b and 3a, 3b demonstrates that they are fully consistent. Thus, the correctness of the simulator operation is proved.

The next step is to consider the operation of the simulator generating the non-Gaussian random process with the three-dimensional probability density of the form

$$w(x_1,x_2,x_3) = \sin(x_1)\sin(x_2)\sin(x_3), \quad 0 \le (x_1,x_2,x_3) \le \pi/2. \tag{14}$$

As it follows from (14), the samples of such a process are uncorrelated. The three-dimensional diagram of the joint probabilities $p(q,k)$ and its level lines are shown in Fig. 9a and Fig. 9b, respectively, while in Fig. 9c the diagram of the matrix of the transition probabilities of the Markov model is presented. One can see that the joint probability diagram is the multimodal one and differs significantly from the Gaussian one. The rows of the matrix of the transition probabilities are the same. This is due to the independence of the adjacent samples, and thus, in this case, the double chain Markov model appears to be redundant.

In Fig. 10, the time realization of the sampling of the simulated random process with the three-dimensional probability density (14) is shown, while Figs. 11a and 11b demonstrate the three-dimensional diagrams of statistical estimates of the matrix of the joint probabilities $p(q,k)$ (Fig. 11a) and its level lines (Fig. 11b) calculated for the sampling with the volume $N > 10^6$. As it can be seen, they are in good agreement with the specified theoretical dependences plotted in Figs. 9a and 9b, respectively.

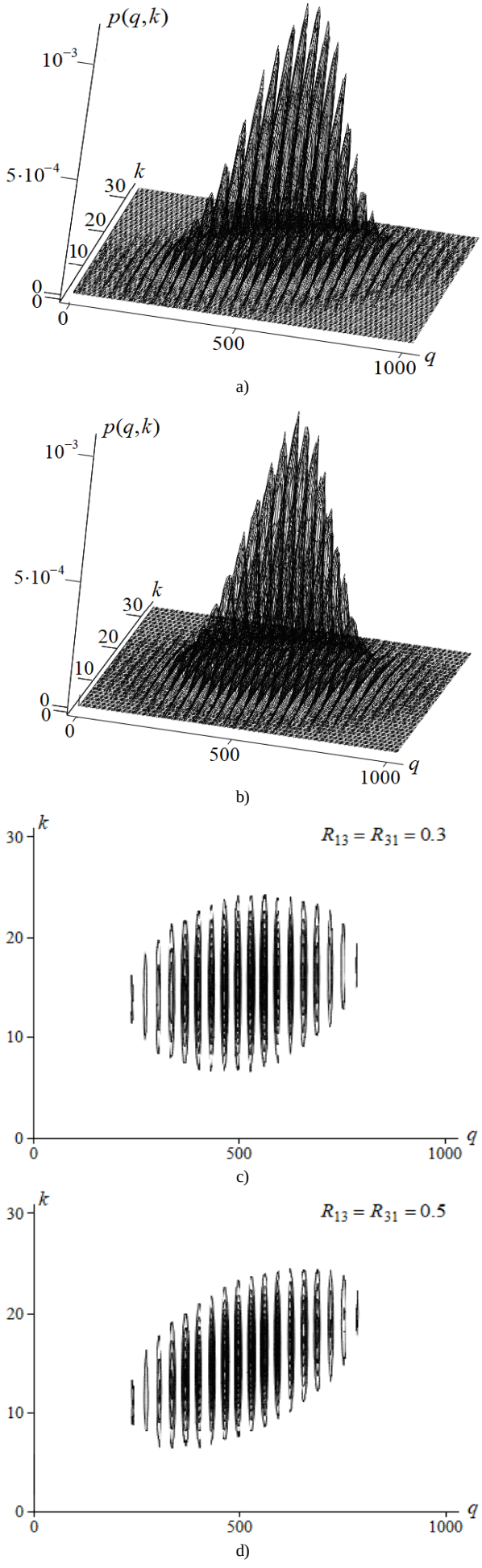

Fig. 8. The diagrams of the experimental probability matrices of the Gaussian random process.

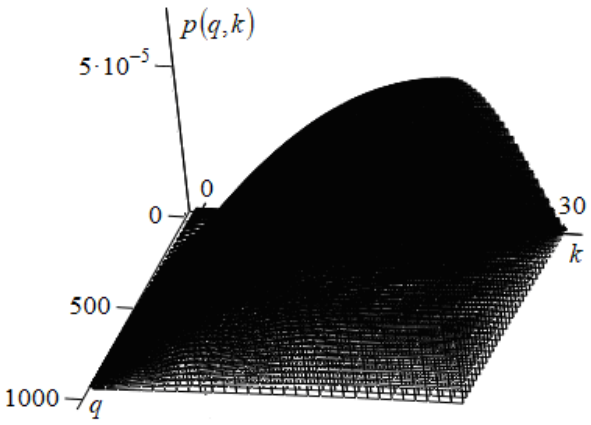

a)

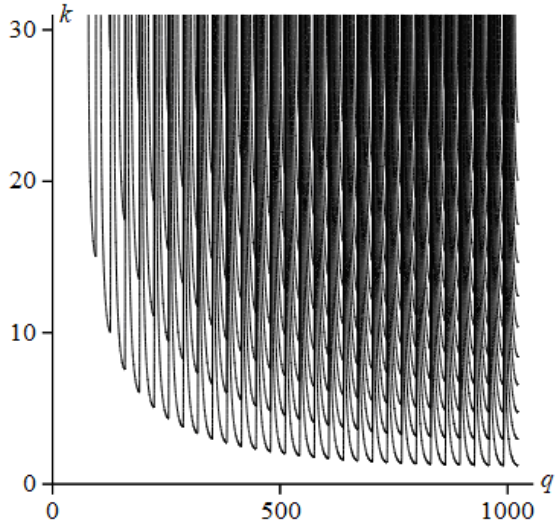

b)

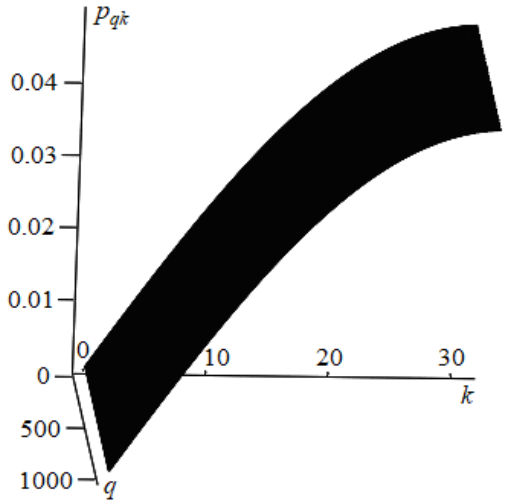

c)

Fig. 9. The diagrams of the probability matrices of the non-Gaussian random process.

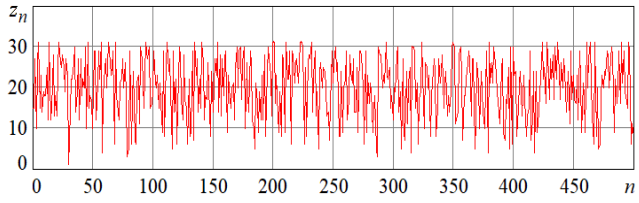

Fig. 10. The time realization of the simulated non-Gaussian random process.

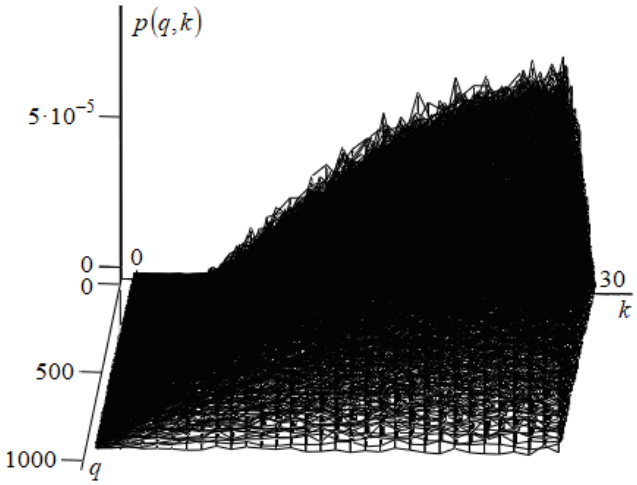

a)

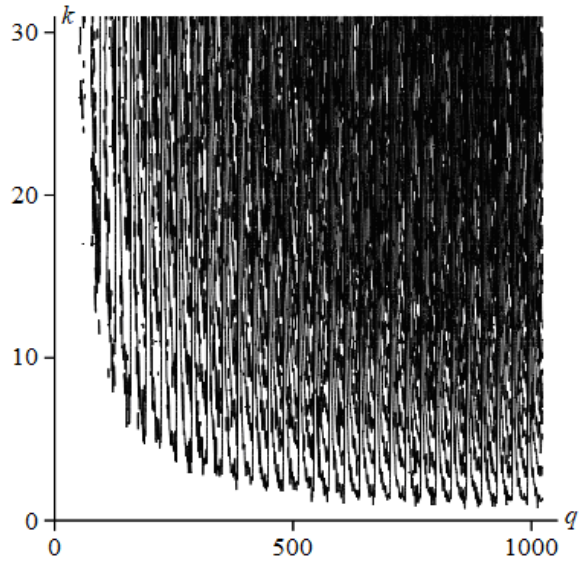

b)

Fig. 11. The diagrams of the experimental probability matrices of the non-Gaussian random process.

It is also of interest to simulate random numbers following the skew normal distribution [9]. In this case, the one-dimensional probability density is determined as follows

$$w(x) = 2\varphi[(x-a)/s]F[b(x-a)/s]/s\,, \tag{15}$$

where

$$\varphi(x) = \frac{1}{\sqrt{2\pi}}\exp\left(-\frac{x^2}{2}\right), \qquad F(x) = \int_{-\infty}^{x}\varphi(t)\,\mathrm{d}t\,,$$

and a is a location parameter, b is a asymmetry parameter, $s>0$ is a scale parameter.

The three-dimensional probability density of the skew normal probability distribution of independent random numbers is

$$w(x_1, x_2, x_3) = w(x_1)w(x_2)w(x_3)\,, \tag{16}$$

while if the random numbers are correlated, then the

specified three-dimensional probability density can be written based on the three-dimensional normal probability distribution (13).

In Fig. 12, the one-dimensional probability density of the skew normal distribution is shown for the case when $s=1$, $a=2$, $b=2$. One can also see the two-dimensional matrices of the transition probabilities $[p_{ij}]$ of the Markov model (Fig. 13a) and the probability distribution function F_{ij} under $M=64$ (Fig. 13b) and the signal sampling range from 0 to 6 with the step of 0.097 (Fig. 13c).

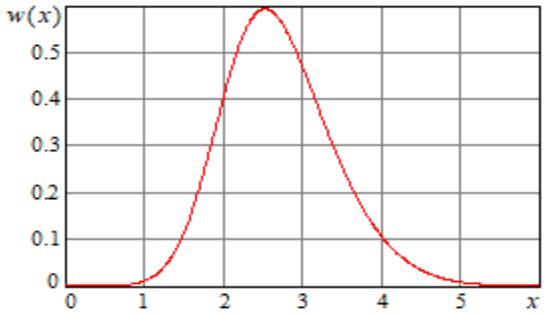

Fig. 12. The one-dimensional probability density of the skew normal distribution.

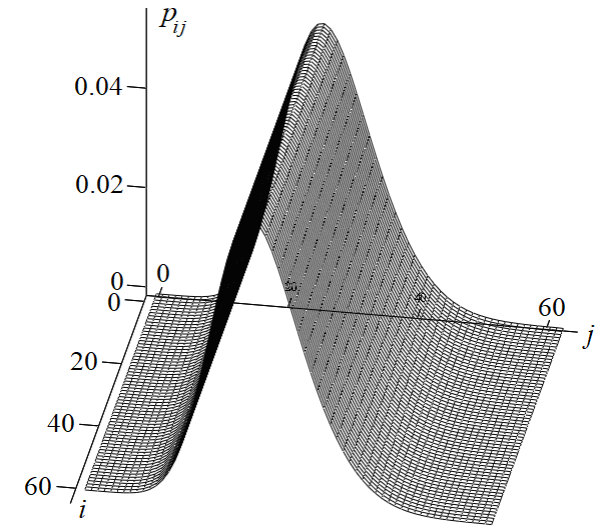

a)

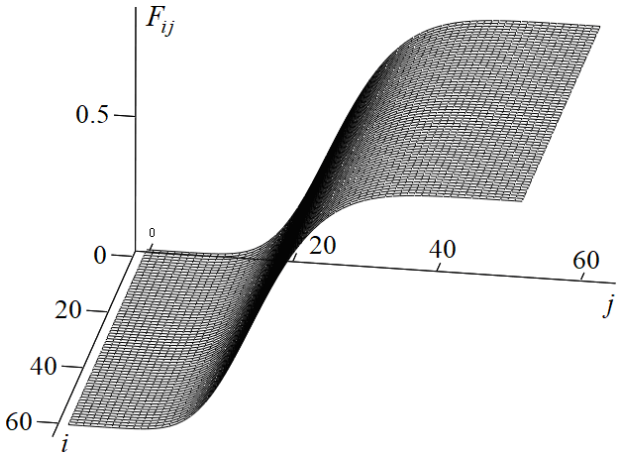

b)

Fig. 13. The two-dimensional matrices of transition probabilities of the Markov model (a) and the probability distribution function (b) of the skew normal random process with the independent samples.

The time has come now to test the proposed simulator capacity for generating independent samples of a random process following the skew normal distribution with the probability densities (15), (16) and the parameters *a*, *b*, *s* assigned above. In Fig. 14, one presents the realization of the samples x_i of such a random process that has been obtained as a result of simulation. In Fig. 15, one can see the values of r_k that is a coefficient of the correlation between the samples x_i and x_j depending on the interval $k=|i-j|$ between them. Finally, in Fig. 16, by the vertical lines, the histogram p_i of the one-dimensional probability distribution of the samples is drawn. In the same Figure, by the dotted line, the theoretical values $\tilde{w}_i=\Delta w(i\Delta)$ of the normalized probability density are plotted for the case when $\Delta=0.1$ (these values have been calculated using the formula (15)). It follows from these Figures that one can maintain a good quality of a random process simulation while applying the introduced algorithm.

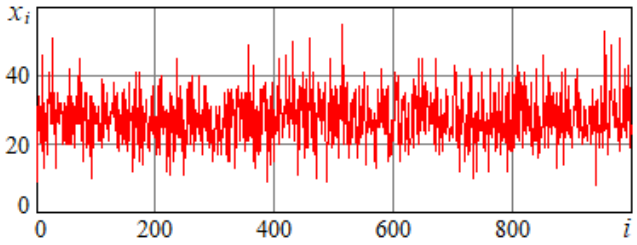

Fig. 14. The time realizations of the simulated skew normal random process with the independent samples.

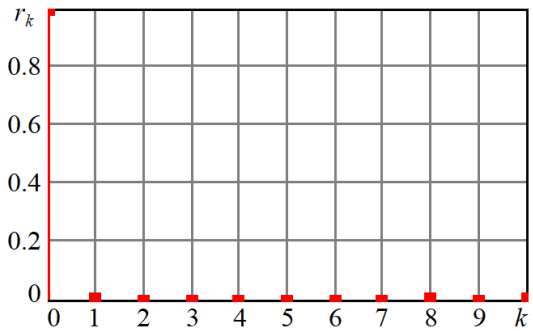

Fig. 15. The correlation coefficient of the simulated skew normal random process with the independent samples.

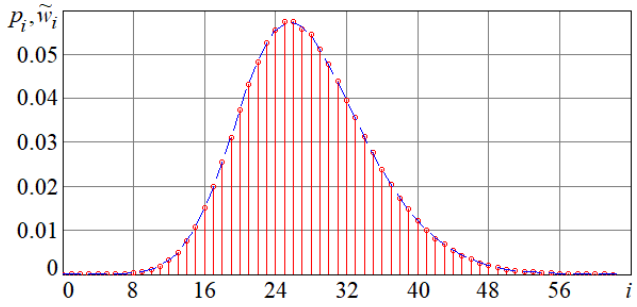

Fig. 16. The histogram and probability density of the simulated skew normal random process with the independent samples.

VII. The Experimental Markov Model

The double chain Markov model of a random process can be built by means of processing of a sufficiently large number of its samples coming from the ADC output connected to the output of a signal source that is, for example, a generator or a radio receiver. As an example, one considers a wideband frequency modulated (WFM) radio signal passed from the output of the radio receiver intermediate frequency path, when the intermediate frequency f_0 is equal to 10.7 MHz while the sampling rate is $f_s = 4f_0$ and $M = 32$ [21].

For a simple Markov model, by using the method similar to one in (13) and then set forth in [21], one can draw a histogram being the empirical two-dimensional probability distribution $p(i, j)$ (the sampling size is 10^7). It is the distribution of the pairs of the samples whose numbers are specified as *i* and *j*, and one can see it in Fig. 17.

According to (13), based on the same sampling, the three-dimensional probability distribution of the "triplets" of the samples whose numbers are specified as *i*, *j*, *k* can be obtained as it is shown in Fig. 18. Here the index *q* is determined in accordance with (3). In Fig. 19, the diagram of the level lines is plotted. One can see from these Figures that the double chain Markov model provides more information about the internal statistical structure of the signal that can be transmitted to its simulator.

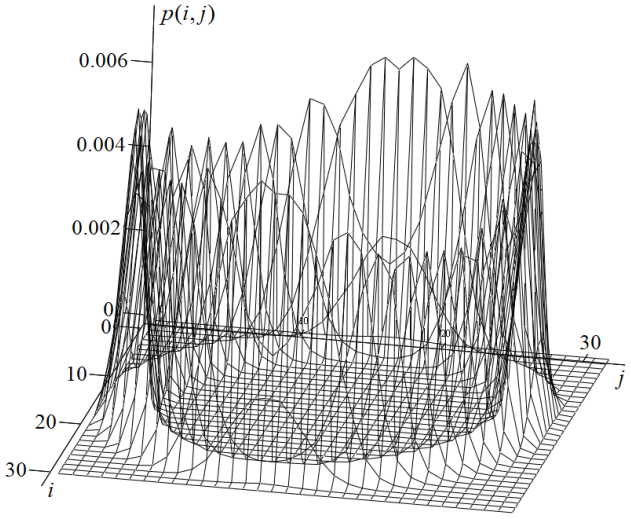

Fig. 17. Simple Markov model of a radio signal.

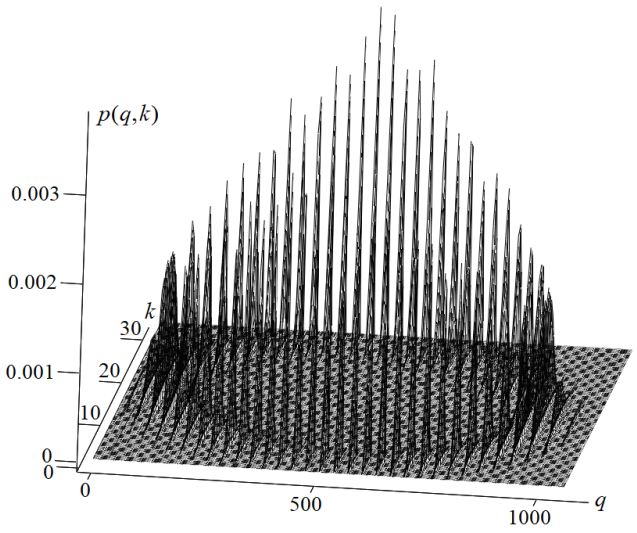

Fig. 18. Double chain Markov model of a radio signal.

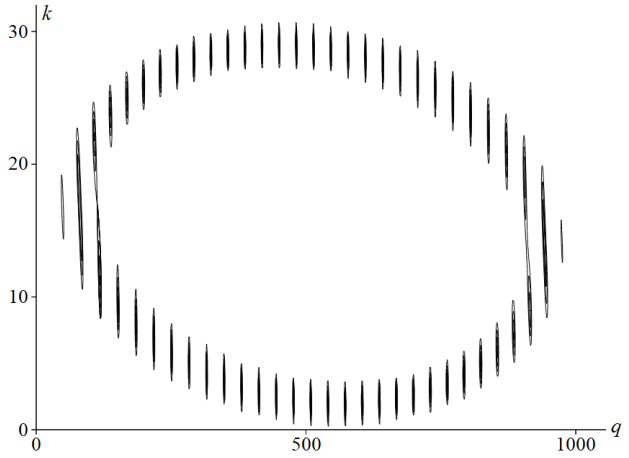

Fig. 19. The diagram of the level lines of the double chain Markov model of a radio signal.

VIII. The Simulator Implementation

The simulator of a random process based on its double chain Markov model can be efficiently implemented by means of microprocessor systems or field-programmable gate arrays [17]. The simulation algorithm allows for a simple software implementation, for example, in the form of a procedure-function.

It follows from (9) that the storage of the Markov model requires the SD having the size of 2^{2m+r} *m*-bit cells. For example, under $m = 8$ and $r = 10$, the operative or permanent (flash) SD is required with a capacity of 64 MB, while under $m = 10$ and $r = 12$, a capacity of 8 GB is required.

If a binary code generator based on a noise generator and a comparator is used as GPSG, then the simulator presented in Fig. 2 generates a random signal in accordance with its double chain Markov model.

IX. Conclusion

The introduced digital simulator of pseudo-random (random) signals that is based on the double chain Markov model displaying the specified three-dimensional probability distribution is universal, high-speed and simple in terms of practical implementation. To change the statistical properties of the generated signal, the new Markov model should be loaded into the memory storage. The model can be built using either the specified three-dimensional probability density of the random process values or the results of statistical processing of the realization of the observed random process of a sufficiently large volume.

The results of statistical simulation of the simulator operation indicate a high accuracy of the generation of the random process realizations possessing the required three-dimensional probabilistic characteristics. The simulator

implementation can be carried out using either specialized software or microprocessor systems and field-programmable gate arrays, and in both cases low computational costs can be ensured.

REFERENCES

[1] D. E. Knuth, *The Art of Computer Programming, Vol. 2. Sorting and Searching*. Boston, Addison-Wesley Professional, 1998.

[2] J. P. C. Kleijnen, *Statistical Techniques in Simulation, Part II*. New York, Marcel Dekker, 1975.

[3] A. M. Law and W. D. Kelton, *Simulation, Modeling and Analysis*. New York, McGraw-Hill Education, 2000.

[4] P. R. Reabody and D. S. Adorno, "Digital synthesis of correlated stationary noise," *Communications of the Association for Computing Machinery*, vol. 5, no. 7, pp. 400-401, 1962.

[5] M. Shinozuka, "Simulation of multivariate and multidimensional random processes," *Journal of the Acoustical Society of America*, vol. 49, no. 1, pp. 556-583, 1971.

[6] P. Cenetobelli, G. Converso, M. Gallo, and L. C. Santillo, "From process mining to process design: a simulation model to reduce conformance risk," *Engineering Letters*, vol. 23, no. 3, pp. 145-155, 2015.

[7] Y. Yu, R. Ru, and K. Fang, "Bio-inspired mobility prediction clustering algorithm for ad hoc UAV networks," *Engineering Letters*, vol. 24, no. 3, pp. 328-337, 2016.

[8] L. E. Varakin, *Communication Systems with Noise-Like Signals* (in Russian). Moscow, Radio i Svyaz', 1985.

[9] D. Ghorbanzadeh, P. Durand, and L. Jaupi, "Generating the skew normal random variable," in *Lecture Notes in Engineering and Computer Science: Proceedings of the World Congress on Engineering 2017*, 5-7 July 2017, London, United Kingdom, pp. 113-116.

[10] X. Zeng, L. Shu, and J. Jiang, "Fuzzy time series forecasting based on grey model and Markov chain," *IAENG International Journal of Applied Mathematics*, vol. 46, no. 4, pp. 464-472, 2016.

[11] W.-K. Ching and M. K. Ng, Markov Chains: Models, Algorithms and Applications. New York, Springer Science, 2006.

[12] A. N. Glushkov, M. Y. Kalinin, V. P. Litvinenko, and Y. V. Litvinenko, "Digital simulator of a random process using Markov model," *Journal of Physics: Conference Series*, vol. 1479, no. 1, paper number 012056, 2020.

[13] O. Chernoyarov, V. Litvinenko, B. Matveev, S. Dachian, and K Melnikov, "The high-speed random number generator with the specified two-dimensional probability distribution," in *Proc. 32nd European Modeling & Simulation Symposium (EMSS)*, Athens, 2020, pp. 16-21.

[14] J. G. Kemeny and J. L. Snell, *Finite Markov Chains*. New York, Springer, 1983.

[15] E. B. Dynkin, *Theory of Markov Processes*. New York, Dover Publications, 2006.

[16] D. Stirzaker, *Stochastic Processes and Models*. Oxford, Oxford University Press, 2005.

[17] C. K. Koc (eds), *Open Problems in Mathematics and Computational Science*. Cham, Springer, 2014.

[18] S. G. Tanyer, "Random number generation with the method of uniform sampling: Very high goodness of fit and randomness," *Engineering Letters*, vol. 26, no. 1, pp. 23-31, 2018.

[19] M. G. Kendall and A. Stuart, *The Advanced Theory of Statistics, Vol. 2: Inference and Relationship*. New York, Hafner Publishing Company, 1973.

[20] M. H. DeGroot, *Optimal Statistical Decisions*. New York, Wiley-Interscience, 2004.

[21] A. N. Glushkov, V. V. Menshikh, N. S. Khohlov, O. I. Bokova, and M. Y. Kalinin, "Markov model based mathematical representation of radio signals," in *Proc. 2nd International Ural Conference on Measurements (UralCon)*, Chelyabinsk, 2017, pp. 239-244.